Dielectric Properties and AC Conductivity of Chitosan-La₂O₃ Nanocomposite

Ali H. Bashal[1] · Mohammed Khalafalla[2] · T. A. Abdel-Basset[2,3]

Abstract

In this study, polymeric films based on chitosan (CS) doped with Lanthanum oxide nanoparticles at different weight percentages (5, 10, 15, and 20% La_2O_3/CS) were prepared using the simple solution cast transformation. The dielectric constant increases with increasing the La_2O_3 content, and this could be attributed to the induced defects, as a result more dipoles are produced in the polymer matrix. Also, the values of Z' and Z'' increase with La contents. On other hand, we noticed that the plot of the normalized-imaginary electric modulus versus the frequency shows a clear peak at high frequency for all samples. This peak is associated with ionic conduction. The AC conductivity increased by increasing the La_2O_3 content. Furthermore, AC conductivity increases with frequency because the absorbed energy from the electric field can increase the number of charge carriers that are participating in the electric conduction. Moreover, the values of the universal exponents were larger than the unity and increase with increasing temperatures which means that the conduction process may be pertinent to reorientational (or localized) mechanism.

1 Introduction

The synthesis of polymer-metal nanostructured materials is becoming an interesting field of research with great impact on the science and technology of materials at the nanoscale [1]. The addition of metal nanoparticles into a polymer matrix is regarded as a feasible means to manipulate and improve the polymer's optical, catalytic, and electronic characteristics.

On the other hand, the internal structure of host polymers can provide an environment for the in situ synthesis and preparation of nanoparticles with different morphologies [2]. Biopolymers, polysaccharide [3–6], and chitosan ([7, 8]) are among the examples of polymers that are used for controlling the synthesis of metal-based nanoparticles. In addition, nanocomposites for various technical purposes can be obtained by the choosing polymers with desirable photoluminescence and conductivity ([9, 10]). Recently, biopolymers have emerged as functional materials for research and industry due to their effective cost, and attractive environmental and ecological impacts. These polymers have intrinsic biological characteristics which make them suitable for various applications in the environmental protection and biotechnology. Generally, composite is having attractive mechanical, thermal, and durability properties that may further be enhanced by modulating their structures at the nanoscale level [11].

Chitosan (CS) is a biopolymer of a polysaccharide type that can be prepared by deacetylation of the chitin. Since the monomer has an amino group and a hydroxyl group, it has excellent chelating and film properties [12]. Therefore, biopolymers are practical matrices for the formation and encapsulation of composites based on the models of metal and semiconductor nanoparticles. The CS is endowed by several merits including, but not limited to, the non-toxicity, high mechanical strength, and several activities in the biology field

✉ T. A. Abdel-Basset
   tmohamed@taibahu.edu.sa

   Ali H. Bashal
   abishil@taibahu.edu.sa

   Mohammed Khalafalla
   mahk74@gmail.com

1 Department of Chemistry, Faculty of Science, Taibah University, Yanbu 46423, Saudi Arabia

2 Department of Physics, Faculty of Science, Taibah University, Yanbu 46423, Saudi Arabia

3 Department of Physics, Faculty of Science, Fayoum University, Fayoum 63514, Egypt

[13]. These advantages have stimulated the use of CS in several fields of applications in chemistry, biology, medicine, pharmaceutical industry, engineering, etc. ([14, 15]).

Electronic material with high dielectric constant (also known as high k materials) is in high demand, due to the fact that they have the potential to be used as a replacement for the silicon dioxide gate insulation which has long been used in the production of silicon-based conventional electronic devices. According to the Moore's law, the electronic devices' size will sustain shrinking into the nanoscale limits and, therefore, silicon dioxide will no longer be capable of coping with this miniaturization process [15]. Nanocomposite materials may play important role in this miniaturization trend. For example, Sagadevan [16] have managed to realize HfO_2/graphene composite structure following a facile synthesis method. This may have a direct impact on the advancement of graphene-based nanoscale devices with efficient HfO_2 gate oxide.

The scope of the size for the gate oxide in future nanodevices will be about 1 nm, requiring a gate insulator with high dielectric constant to provide the same insulation quality as that is for the silicon oxide in conventional devices [15].

Some of the potential candidates for the replacement of silicon dioxide as the gate dielectrics in future electronic technology are Zirconium oxide [17], and lanthanum oxide [18]. Lanthanum oxide has a large dielectric constant [19], wide band-gap [20], and thermodynamically stability when deposited on silicon [21]; hence, it acts as an attractive dielectric for future electronic technology.

Chitosan's ability to form compounds with lanthanum ions arises from the NH2 group present in the glucosamine b unit (1–4) of the polymer. Its hydroxyl groups also interact with the metal ions, but to a lesser extent [22]. Also, the complexity of the mineral ions in the chitosan chain changes their properties [22, 23] or offers a completely new function [24]. As far as we know, there are no previous reports on the dielectric and conductive properties of lanthanum oxide chitosan complexes.

In this paper, different percentages of lanthanum oxide were loaded on chitosan thin film for the purpose of investigating the effect of the metal oxide on the dielectric and AC conductivity properties of the chitosan. The temperature dependence of the properties of lanthanum oxide-doped chitosan thin films was also investigated.

2 Experimental

2.1 Materials and Methods

Chitosan (powder, shrimp shells, product no. C3646, density = 0.15–0.3 g/cm^3) and La_2O_3 (nano powder, < 100 nm par-

ticle size TEM, product no. 634271) were purchased from Sigma-Aldrich company.

2.2 Preparation of CS-La$_2$O$_3$ Nanocomposite Film

1% chitosan solution was prepared by dissolving chitosan in 1% (w/v) aqueous acetic acid solution under stirring overnight. The formed viscous solution was filtered, and 5, 10, and 15 (w/v %) of La_2O_3 was added portion-wise under vigorous stirring; the stirring was continued for additional 24 h. A sample of 20 g of the obtained solution was poured into Teflon petri-dish (8 cm) and dried in the vacuum oven adjusted at 50 °C for 3 days to remove the solvent. Chitosan-La_2O_3 nanocomposite film was peeled off from the petri-dish after neutralization with 5 mL of 1 M NaOH and then was rinsed with distilled water. Finally, the produced film was kept inside a vacuum desiccator at room temperature for 2 days.

2.3 Measuring Dielectric Properties

We used "Solartron Frequency and Analytical Response analyzer" instrument for measuring the impedance spectra associated with our samples that were in the form of circular thin films, ~ 0.1 mm thick and ~ 0.5 cm in radius. The samples were connected in series with small 47 Ω resistor to stabilize the signal. The measurement frequency range was $f = 0.1$ kHz $- 0.3$ MHz at an AC amplitude of 0.3 V and zero DC voltage.

We used copper tapes as the electrodes that were fixed on the samples with a thin layer of adhesive (conductive adhesive with negligible contribution to the impedance) to avoid using a conducting paste (available to us was a silver paste) that would diffuse into the sample, resulting into unwanted signal in the impedance spectrum (Fig. 1).

3 Results and Discussion

3.1 Dielectric Properties of chitosan-La$_2$O$_3$ Nanocomposite

The dependence of the dielectric constant, ε', on frequency for various La_2O_3 compositions (5–20%) at room temperature is shown in Fig. 2a.

The dielectric constant decreases rapidly at low frequencies and then gets saturated at higher frequencies (~ > 10 k Hz) indicating the rotational motion of the polar molecules of the dielectric is not sufficiently rapid for the attainment of equilibrium with the field. The sharp reduction in ε' (Fig. 2a) suggests the formation of space charge polarization at the sample-electrode interface (possibly associated with C1 and R1 in the equivalent circuit, Fig. 3a).
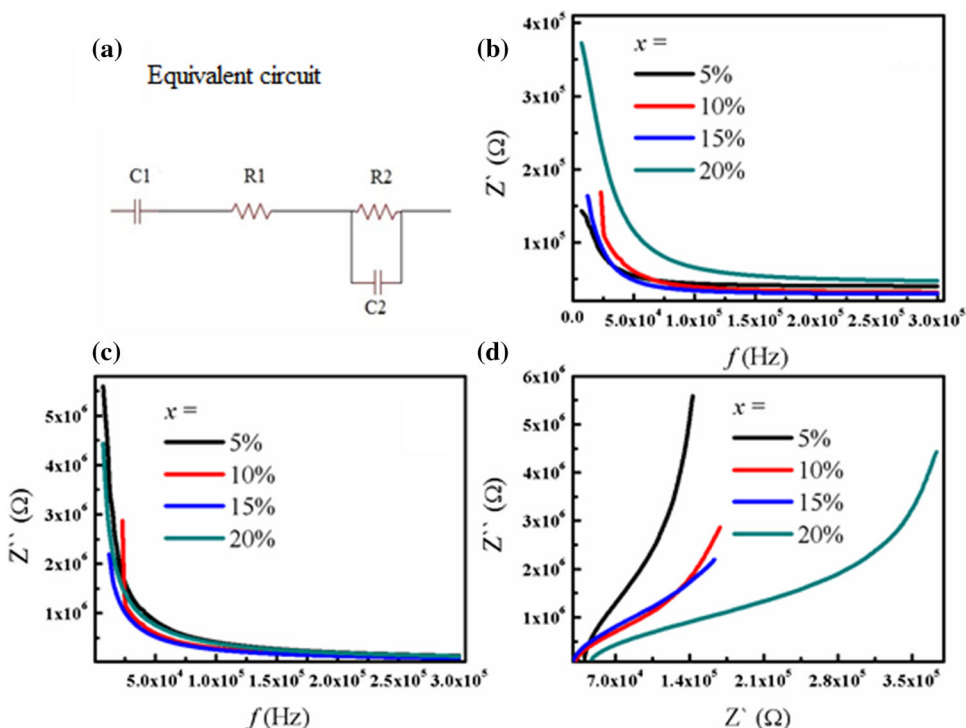
Fig. 1 Conversion of chitosan to chitosan-La$_2$O$_3$ nanocomposite
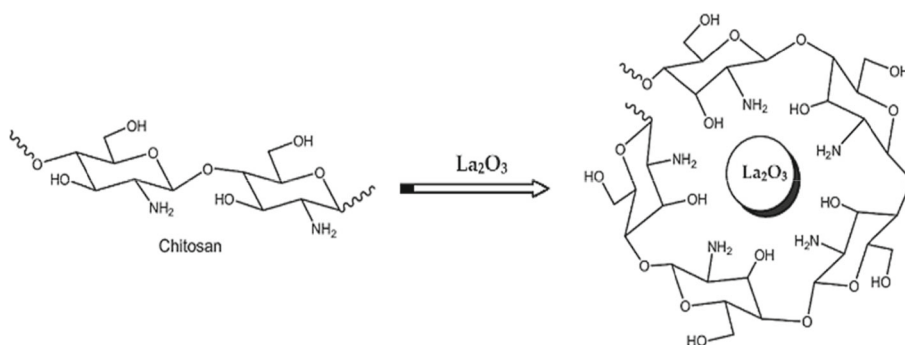
Fig. 2 Frequency dependence of dielectric permittivity ε' and dielectric loss ε'' for (La$_2$O$_3$)$_x$/CS at room temperatures
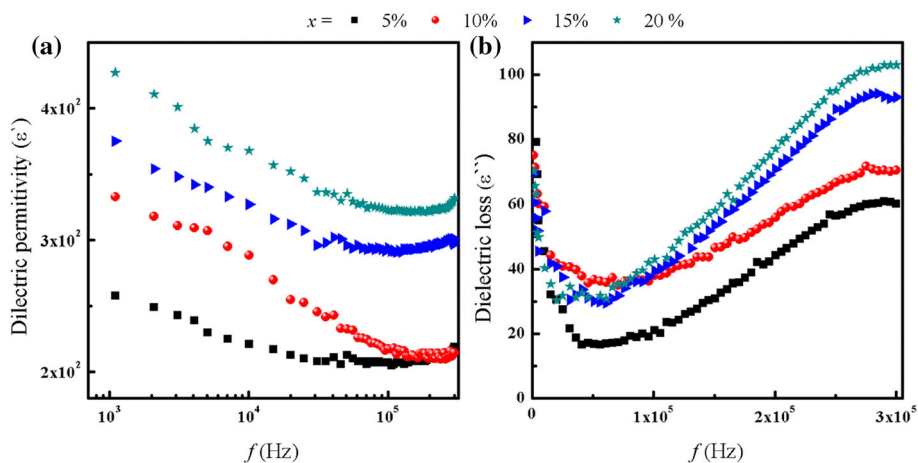
Fig. 3 **a** The equivalent circuit, variation of **b** Z' and **c** Z'' with frequency and **d** Z' with Z'' for (La$_2$O$_3$)$_x$/CS

This is a large area interface with relatively large capacitance and hence, has relatively large relaxation time for the charge polarization induced by the AC signal. Consequently, those charges cannot follow the electric field oscillation at high frequency where processes with smaller time constants would emerge. Charge hopping between La$_2$O$_3$ sites may

Table 1 The values of the fitting parameters for $(La_2O_3)_x$/CS

| X %	The fitting parameters				
	C1 (pF)	R1 (MΩ)	C2 (pF)	R2 (MΩ)	τ = (μs)
5	4.0458	0.040165	72.835	0.11721	8.537
10	6.331	0.031384	38.692	0.20800	15.150
15	6.9259	0.029198	44.170	0.22071	9.749
20	5.1085	0.044826	18.633	0.30892	5.756

also contribute to the dielectric properties. However, the hopping process is saturated at high frequencies because the charge exchange rate between the sites cannot match the high signal frequency. Also, it is observed that the dielectric constant increases with increasing the La_2O_3 content which is attributed to Maxwell–Wegner ionic conduction [25]. The typical behavior of the ε' has been recognized for all investigated samples like the earlier reports for Chitosan/nano-ZnO composite films [26].

Another important characteristic of the electrical insulation is dielectric loss, ε''. Figure 2b shows the dielectric loss behavior of chitosan with different La_2O_3 contents at room temperature as a function of frequency. Relaxation peaks are observed at high temperatures, especially for $(La_2O_3)_x$/CS. This peak is defined as the α-relaxation related to the kinetics of the chitosan segments. The dispersion observed in the low-frequency ε'' spectrum is accompanied by an increase in ε' (Fig. 2a). This reveals the formation of space charge regions (polarization at the sample-electrode interface) [27].

The equivalent impedance circuit model shown in Fig. 3a consists of a contact capacitor (C1) in series with a resistor, R1, and R2-C2 parallel resistor–capacitor circuit by using the EIS Spectrum Analyzer. Figure 3b,c shows the variation in Z' and Z'' with frequency, it was found that the magnitude of Z' decreases gradually with frequency which indicates possible release of space charge concomitant with the reduction in resistive properties of the materials, Similar behavior was reported earlier for TiO2 doped PVA/CN-Li [28]. Also, the Z'' has the same trend to Z'. The magnitude of Z' and Z'' increased with the La contents, which is attributed to the decreasing grain size values. This indicates that the decrease in conduction path is due to the hindrance posed by grain boundaries. Figure 3 shows the variation of Z'' versus Z' for all the samples. It can be notice that the ionic resistance of $(La_2O_3)_x$/CS decreases with increasing the La content.

Table 1 shows the values for the parameters R1, R2, C1, and C2 used to fit the experimental data. The time constant T = R2*C2 that is expected to be associated with the transport mechanism of charge carriers in the bulk chitosan that is influenced by La concentration. Overall, one can roughly notice that τ reduces as the La percentage increases, which reflects the metallic nature of the La transport sites.
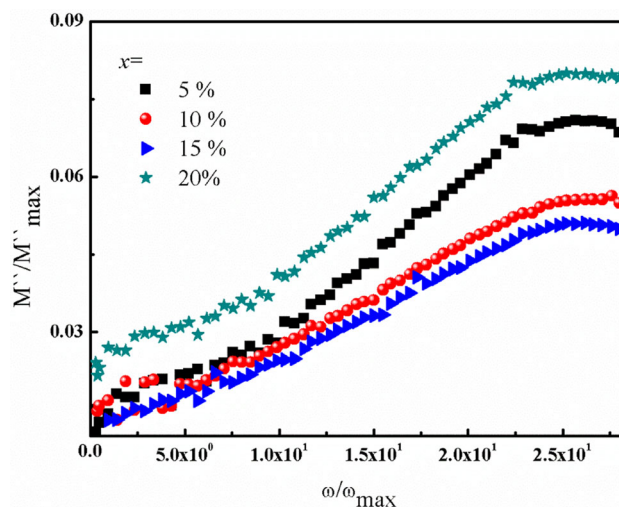
Fig. 4 The variation of dielectric spectra of M''/M''_{max} with w/w_{max} at room temperature for $(La_2O_3)_x$/CS

To overcome the problem of the interfacial polarization intervention in our data, the electric modulus, M^*, approach has been employed to study the conductivity data in polymer composites to suppress the electrode polarization effect. The electric modulus takes the form [29].

$$M^* = M' + M'' \tag{1}$$

Where M' and M'' are the real and imaginary parts of the electric modulus, and given by

$$M' = \frac{\varepsilon'}{\varepsilon'^2 + \varepsilon''^2}, M'' = \frac{\varepsilon''}{\varepsilon'^2 + \varepsilon''^2}, \tag{2}$$

Figure 4 shows the dielectric spectra of the normalized-imaginary part of the electric modulus, M''/M''_{max}, as a function of the normalized angular frequency w/w_{max}, measured at room temperature. The values of M'' tend to be zero at low frequency which indicates the removal of the electrode polarization for the investigated samples. As clear peak appears at high frequency for all sample which may be attributed to the electric conduction of ions [29]. The AC conductivity dependence of frequency can be calculated by $(\sigma_{ac} = \omega\varepsilon_0\varepsilon tan\delta)$, where ω is the angular frequency, ε_0 is the permittivity of the free space and tan δ is loss tangent.

The frequency dependence of σ_{ac} for the $(La_2O_3)_x$/CS composites at room temperature is shown in Fig. 5. Clearly, the increase in the AC conductivity by increasing frequency indicates that the charge carriers transport is dominated by hopping between defect sites along the chains [30], agreeing with the dielectric constant data shown in Fig. 1. The distribution of La_2O_3 allows the formation of conductive paths throughout the networks of the composite, which contributes

Table 2 The values of the exponent s for $(La_2O_3)_x$/CS at room temperatures

X %	5	10	15	20
s	1.988	1.64	1.955	1.92

to the polaron and charge carriers hopping between the localized states.

It is also obvious that the conductivity is enhanced by the increase in the La_2O_3 content. The conductivity σ_{ac} also increases with the frequency, which may be due to the increase in the absorbed energy from the electric field which increases the number of charge carriers contributing to the conduction process.

$(\sigma_{ac} = B\omega^s$

The AC conductivity dependence of frequency is given by $(\sigma_{ac} = B\omega^s$, where s is the universal exponent, to determine the type of the conduction mechanism for $(La_2O_3)_x$/CS. The variation of $ln(\sigma_{ac})$ versus ln (f) at room temperatures is shown in Fig. 5, and the values of s are listed in Table 2.

We show that the values of s were larger than unity and increase with La_2O_3 content. This means that the conduction mechanism may be attributed to the localized/reorientation processes [31].

The activation energy (E_a) for 5% La_2O_3/CS composite was calculated by Arrhenius relation $\sigma_{ac} = \sigma_o exp\left(\frac{-E_a}{kT}\right)$. The AC conductivity (ln σ_{ac}) as a function of (1000/T) is shown in Fig. 6. It is clear that σ_{ac} increases with temperature. This is due to the increase in the absorbed energy which leads to an increase in the number of the charge carriers that are responsible for the conduction process. The values of E_a at f = 5 kHz to 0.3 MHz are summarized in Table 3.

It is observed that the values of E_a are increased with increasing the frequency which leads to an increase in the number of free charge carriers.

As seen from Table 3, the E_a values are very small (0.017–0.109 eV) suggesting charge carrier hopping between localized states. The low values of the activation energy may indicate the existence of a transitional regime between hopping and another conduction process possibly due to free
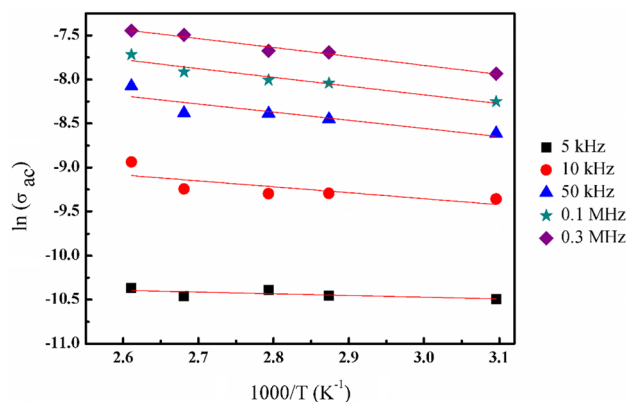
Fig. 6 The AC conductivity (ln σ_{ac}) as a function of (1000/T) for 5% La_2O_3/CS at fixed frequencies

**Table 3** The values of the activation energy, E_a for (5% La_2O_3/CS) at fixed frequencies

F (Hz)	5 k	10 k	50 k	0.1 M	0.3 M
E_a (eV)	0.017	0.059	0.082	0.088	0.11

band conduction. Thus, these values may be attributed to the presence of ionic conduction mechanism in our samples.

4 Conclusion

The chitosan-La_2O_3 nanocomposite film has been synthesized by incorporating La_2O_3 nanoparticles within the chitosan matrix using the solution cast method. The dielectric constant increases with increasing La_2O_3 content. This could be attributed to the induced defects, which produce more dipoles in the polymer matrix. Furthermore, the increase in dielectric constant and loss reflects the increase in the number of free ions in the polymer matrix. In addition, the values of Z' and Z'' increase with La contents, in other hand, the time constant τ reduces as La percentage increases, which reflects the metallic nature of the La transport sites. Moreover, the

Fig. 5 a frequency dependence of σ_{ac}, and **b** the variation of ln (σ_{ac}) dependence of frequency for $(La_2O_3)_x$/CS at room temperatures, and the solid line is the fitting according
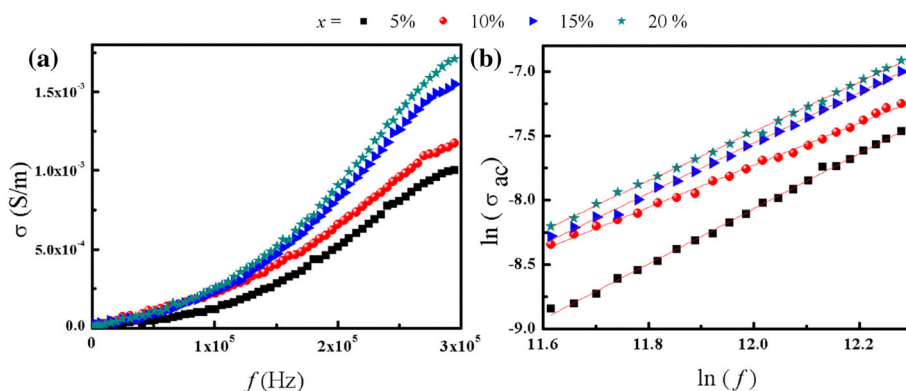
increase in the AC conductivity with increasing La_2O_3 content and frequency might be associated with the increase in the absorbed energy from the electric field. The conduction mechanism might be attributed to localized/reorientational processes judging from the values of the exponent s (from the fitting of the conductivity vs. frequency to the power law) which were higher than unity and increased with increasing the temperatures. Regarding the activation energies, their values have increased with increasing the frequency, leading to an increase in the number of the free charge carriers.

References

1. Pomogailo, A.D.; Kestelman, V.N.: Metallopolymer nanocomposites, vol. 81. Springer, Berlin (2006)

2. Lu, Q.; Gao, F.; Komarneni, S.: A green chemical approach to the synthesis of tellurium nanowires. Langmuir **21**(13), 6002–6005 (2005)

3. Wang, C. et al.: Thermoresponsive starch-based particle-stabilized Pickering high internal phase emulsions as nutraceutical containers for controlled release. Int. J. Biol. Macromol. **1**(146), 171–178 (2020)

4. Olatunji, O.: Starch. In: Aquatic Biopolymers. Springer, Berlin, pp. 287–310 (2020)

5. Xiong, Y., Huang, L., Mahmud, S., Yang, F., Liu, H.: Biosynthesized palladium nanoparticles using alginate for catalytic degradation of azo-dyes. Chin. J. Chem. Eng.**28**(5), 1334–1343 (2020)

6. Ambrogi, V. et al.: Biocompatible alginate silica supported silver nanoparticles composite films for wound dressing with antibiofilm activity. Mater. Sci. Eng. C. **112**, 110863 (2020)

7. Shih, C.-M.; Shieh, Y.-T.; Twu, Y.-K.: Preparation of gold nanopowders and nanoparticles using chitosan suspensions. Carbohydr. Polym. **78**(2), 309–315 (2009)

8. Wei, D.; Qian, W.; Wu, D.; Xia, Y.; Liu, X.: Synthesis, properties, and surface enhanced Raman scattering of gold and silver nanoparticles in chitosan matrix. J. Nanosci. Nanotechnol. **9**(4), 2566–2573 (2009)

9. Balamurugan, A.; Ho, K.-C.; Chen, S.-M.: One-pot synthesis of highly stable silver nanoparticles-conducting polymer nanocomposite and its catalytic application. Synth. Met. **159**(23–24), 2544–2549 (2009)

10. Yang, J. et al.: Development of aliphatic biodegradable photoluminescent polymers. Proc. Natl. Acad. Sci. **106**(25), 10086–10091 (2009)

11. Thostenson, E.T.; Li, C.; Chou, T.-W.: Nanocomposites in context. Compos. Sci. Technol. **65**(3–4), 491–516 (2005)

12. Gao, H.; Liu, N.; Ni, S.; Lin, H.; Fu, Y.: Xylan/chitosan composites prepared by an ionic liquid system with unique antioxidant properties. J. Bioresour. Bioprod. **2**(3), 100–104 (2017)

13. Wang, B. et al.: Chitosan-mediated synthesis of gold nanoparticles on patterned poly (dimethylsiloxane) surfaces. Biomacromol **7**(4), 1203–1209 (2006)

14. Yi, H. et al.: Biofabrication with chitosan. Biomacromol **6**(6), 2881–2894 (2005)

15. Buchanan, D.A.: Scaling the gate dielectric: materials, integration, and reliability. IBM J. Res. Dev. **43**(3), 245–264 (1999)

16. Sagadevan, S.; Chowdhury, Z.Z.; Johan, M.R.B.; Rafique, R.F.: A facile one-step hydrothermal synthesis of HfO2/graphene nanocomposite and its physio-chemical properties. Mater. Res. Express **5**(3), 035014 (2018)

17. Kukli, K.; Ritala, M.; Leskelä, M.: Low Temperature Deposition of Zirconium Oxide-Based Nanocrystalline Films by Alternate Supply of Zr [OC (CH3) 3] 4 and H2O. Chem. Vap. Depos. **6**(6), 297–302 (2000)

18. Stemmer, S.; Maria, J.-P.; Kingon, A.: Structure and stability of La 2 O 3/SiO 2 layers on Si (001). Appl. Phys. Lett. **79**(1), 102–104 (2001)

19. Rao, U.S.; Kumar, J.S.; Reddy, K.N.: Nucleation, growth and characterization of thin solid films. Prog. Cryst. Growth Charact. **15**(3–4), 187–314 (1987)

20. Evarestov, R.; Leko, A.; Petrov, A.; Veryazov, A.: Electronic structure of La, O, and LaF, crystals. Phys. Stat. Solb. **170**, 145 (1992)

21. Hubbard, K.; Schlom, D.: Thermodynamic stability of binary oxides in contact with silicon. J. Mater. Res. **11**(11), 2757–2776 (1996)

22. Guibal, E.: Interactions of metal ions with chitosan-based sorbents: a review. Sep. Purif. Technol. **38**(1), 43–74 (2004)

23. Varma, A.; Deshpande, S.; Kennedy, J.: Metal complexation by chitosan and its derivatives: a review. Carbohydr. Polym. **55**(1), 77–93 (2004)

24. Bhatia, S.C.; Ravi, N.: A magnetic study of an Fe − chitosan complex and its relevance to other biomolecules. Biomacromol **1**(3), 413–417 (2000)

25. Hdidar, M.; Chouikhi, S.; Fattoum, A.; Arous, M.; Kallel, A.: Influence of TiO2 rutile doping on the thermal and dielectric properties of nanocomposite films based PVA. J. Alloys Compd. **750**, 375–383 (2018)

26. Rahman, P.M.; Mujeeb, V.A.; Muraleedharan, K.; Thomas, S.K.: Chitosan/nano ZnO composite films: enhanced mechanical, antimicrobial and dielectric properties. Arab. J. Chem. **11**(1), 120–127 (2018)

27. Abou Elfadl, A.; Ismail, A.; Mohammed, M.: Dielectric study and AC conduction mechanism of gamma irradiated nano-composite of polyvinyl alcohol matrix with Cd 0.9 Mn 0.1 S. J. Mater. Sci.: Mater. Electron. **31**(11), 8297–8307 (2020)

28. Zhu, Y.; Hua, Y.; Zhang, S.; Wang, Y.; Chen, J.: Open-cell macroporous bead: a novel polymeric support for heterogeneous photocatalytic reactions. J. Polym. Res. **22**(4), 57 (2015)

29. Shakoor, A.; Rizvi, T.Z.; Saeed, M.: Dielectric properties of polypyrrole/pillared clay nanocomposites. Polym. Sci. Ser. A **54**(5), 401–406 (2012)

30. Shakoor, A.; Rizvi, T.Z.; Nawaz, A.: Raman spectroscopy and AC conductivity of polyaniline montmorillonite (PANI–MMT) nanocomposites. J. Mater. Sci.: Mater. Electron. **22**(8), 1076–1080 (2011)

31. Abdel-Baset, T.; Hassen, A.: Dielectric relaxation analysis and Ac conductivity of polyvinyl alcohol/polyacrylonitrile film. Phys. B Condens. Matter **499**, 24–28 (2016)